

Shaorui ZHOU, Jia PAN, Min ZHAO, Lingxiao WU, Weiqing LI

# Data-driven vertiport location optimization for urban air mobility

© The Author(s) 2026

**Abstract** Urban air mobility (UAM), as an emerging transportation mode, represents an effective strategy to alleviate ground traffic congestion and is expected to be promoted globally in the coming years. This study focuses on the data-driven optimization of vertiport location. By integrating travel choice modeling with a three-phase multi-objective integer programming (TP-MOIP) model based on  $K$ -means clustering analysis, the study provides decision-making support for scientific vertiport network planning. The study combines revealed preference (RP) and stated preference (SP) surveys, employing binomial logistic regression to analyze the probability of individuals choosing UAM, while introducing time value coefficients to identify potential user groups. Utilizing ride-hailing order data, potential vertiport locations were identified through  $K$ -means clustering. The developed TP-MOIP model simultaneously optimizes the objectives of demand coverage maximization and cost minimization across three implementation phases. Using Shenzhen as a case study, the feasibility of the proposed approach was validated. The results show that the average selection probability for

UAM is 16.7%, with time-sensitive users being a critical demographic. In addition, the TP-MOIP model achieved a demand coverage rate of 88.21%. Sensitivity analysis indicates that the land cost budget has the most pronounced impact on demand coverage. This research establishes both theoretical foundations and practical methodologies for vertiport location optimization, offering substantial implications for advancing UAM development.

**Keywords** urban air mobility (UAM), travel choice modeling, clustering algorithm, vertiport location optimization

## 1 Introduction

The Advanced Air Mobility (AAM) Ecosystem refers to economic activities such as commerce, public services, and personal consumption conducted using various low-altitude aircraft within airspace below 1,000 m. Advancements in drone technology, improvements in flight control systems, and adjustments in airspace management policies are all driving the expansion of the AAM Ecosystem from its traditional roles in military reconnaissance and surveillance to broader applications, such as agriculture, logistics, and urban transportation. With the intensification of traffic congestion in urban and suburban areas, the ground driving time required for people's commutes is constantly increasing. During peak hours, traffic congestion at a single intersection can cause an economic loss of CNY 1,277 per hour and generate 238 kg of CO<sub>2</sub> emissions in a typical Chinese metropolitan area (AutoNavi, 2024). This congestion not only results in additional travel time, but also leads to reduced efficiency and lost productivity (Falcochio and Levinson, 2015). Furthermore, studies show that prolonged driving time significantly increases pollutant emissions, exacerbating air pollution and climate change, which may ultimately trigger public health crises (Nadrian et al., 2019). Given these challenges, there is an urgent need to explore alternative transportation modes. UAM is regarded as an

---

Received Sep. 29, 2025; revised Jan. 21, 2026; accepted Feb. 4, 2026

Shaorui ZHOU, Jia PAN, Weiqing LI  
School of Intelligent Systems, Sun Yat-sen University, Guangzhou 510275, China

Min ZHAO  
Faculty of Business Administration, E22, University of Macau, Macao Special Administrative Region 999078, China

Lingxiao WU (✉)  
Department of Aeronautical and Aviation Engineering, Hong Kong Polytechnic University, Hong Kong Special Administrative Region 999077, China  
E-mail: lingxiao-leo.wu@polyu.edu.hk

This work was supported by the National Natural Science Foundation of China (Grant No. 72271251), the Natural Science Foundation of Guangdong Province, China (No. 2023A1515010683), Guangzhou Municipal Science and Technology Program (No. 2025B01J0002), China.

Open access funding provided by The Hong Kong Polytechnic University.

effective strategy to alleviate traffic congestion in large metropolitan areas due to its unique airspace utilization capability and significant emission reduction effect (Yan et al., 2024; Du et al., 2025).

The concept of UAM originates from the idea of “flying cars,” and later NASA proposed a formal definition: a system that uses Vertical Take-Off and Landing (VTOL) aircraft to build an air traffic route network in dense urban environments, with the goal of playing an important role in future urban and intercity transportation (Goyal et al., 2018). UAM can be categorized into passenger services, cargo services, and other services according to application demands (Cohen et al., 2021). Among these, passenger services have evolved into two main operational modes: air shuttle service and air taxi service (Long et al., 2023). Initially, air shuttle services were operated as “corridor services” (Bauranov and Rakas, 2021), primarily operating on fixed routes, such as those connecting airports and city centers. As demand increased, the system has evolved into a hub-and-spoke network centered on vertical transportation hubs, which connects neighboring vertiports through radial routes and reduces operating costs via regularly scheduled shared flights. Air taxi services provide near-point-to-point on-demand services utilizing infrastructure of various sizes based on urban density and flight demand. As shown in Fig. 1, the whole process of air taxi service is divided into three main phases: (i) from origin to initial vertiport, (ii) between initial and target vertiports, and (iii) from target vertiport to final destination (Rajendran and Srinivas, 2020). The European Aviation Safety Agency (EASA) established the world’s first regulatory framework for urban air taxi operations (European Union Aviation Safety Agency, 2022). Dubai stands as one of the global pioneers in air taxi pilot programs. In 2017, the Dubai Roads and Transport Authority (RTA) collaborated with Volocopter to conduct the world’s first test flight of an autonomous air taxi. In 2019, Singapore initiated an air taxi pilot program in partnership with Volocopter, completing multiple successful test flights. The Federal Aviation Administration (FAA) granted approval to Joby Aviation’s air taxi initiative in 2023, authorizing experimental flight operations (Joby Aviation, 2024). In China,

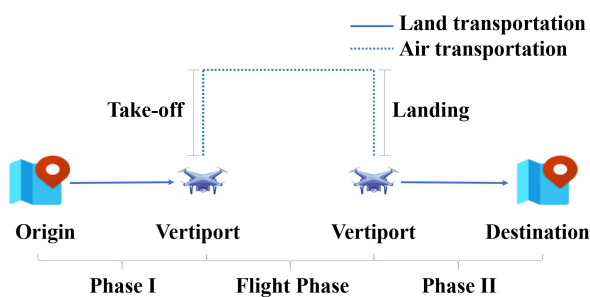


Fig. 1 Process of air taxi service.

EHang Intelligent established a 5G-enabled UAM Experience Center in Guangzhou, deploying an operational base for autonomous aerial vehicles.

Although UAM pilot programs have advanced rapidly worldwide, megacities face unique implementation challenges due to their high population density and complex traffic structures. This study aims to support decision-making in optimizing vertiport placement in megacities and to promote the sustainable development of UAM. To achieve this goal, we focus on travel choice modeling, demand estimation, and vertiport location optimization for UAM systems, using Shenzhen as a case study. The main contributions of this work are as follows:

1) In terms of travel choice modeling, this study innovatively combined two survey methods, RP and SP, and collected the acceptance of and willingness to pay for UAM services among high-net-worth individuals through 1,386 valid questionnaires. The study analyzed the probability of individuals choosing UAM using a binomial logistic regression model. The results showed that the average selection probability was 16.7%, indicating that UAM, as an emerging mode of transportation, has viable market potential. The research innovatively introduced the concept of the time value coefficient. By quantifying an individual’s trade-off between time cost and monetary cost, it identified potential user groups with high time sensitivity, providing important data for subsequent demand analysis and location selection.

2) Regarding the location optimization problem, this study proposes a TP-MOIP model based on spatial clustering. The study first employed the  $K$ -means algorithm for OD point cluster analysis. The final silhouette coefficient was 0.43 and the DBI was 0.77, indicating good clustering quality. The subsequently constructed TP-MOIP model innovatively utilizes an improved weighted synthesis method, transforming the dual objectives of demand coverage maximization and operating expense minimization into a single objective function, while incorporating a phased optimization mechanism to reflect UAM network construction dynamics. Model results demonstrate that with weight parameter  $\hat{a} = 0.8$ , the three-phase implementation achieves 88.21% demand coverage.

3) Through sensitivity analysis, this study systematically evaluated the impact of key parameters such as land cost, labor cost, and transportation accessibility on demand coverage. The research finds that the land cost budget has a significant positive impact on the demand coverage rate, and its sensitivity increases as the construction stage progresses. The labor cost budget and transportation accessibility constraints have obvious phase-specific characteristics. The monotonicity in the early phase may cause abnormal phenomena, but the demand will be met in the subsequent phase.

The remainder of this paper is organized as follows. Section 2 presents a review of the literature. Section 3

analyzes travel choice behavior using survey data. Section 4 proposes a vertiport location model with a *K*-means clustering algorithm. Section 5 conducts systematic sensitivity analysis on key model parameters. Section 6 summarizes the main findings obtained in this paper.

## 2 Literature review

This section presents the literature of travel choice modeling, UAM demand estimation and vertiport siting optimization.

### 2.1 Travel choice modeling

Existing research indicates that the demand for UAM is influenced by multiple factors. Ugur Eker et al. (2020) conducted online questionnaire surveys and statistical analyses, revealing that public acceptance of UAM was significantly affected by demographic characteristics, travel behavior patterns, and subjective attitudes. Similarly, Boddupalli et al. (2019) surveyed 2,500 commuters in six major metropolitan areas (including Atlanta) and found that, in addition to travel time and cost, service frequency and ground transportation conditions also significantly influenced UAM demand. As shown in Table 1, a synthesis of existing studies suggests that the key demand factors for UAM can be summarized into three main categories: individual user characteristics, service supply characteristics, and external environmental conditions.

Individual user characteristics include subjective acceptance and objective demographic characteristics. The Technology Acceptance Model (TAM) proposed by Davis et al. (1989) provides a theoretical basis for such research, which predicts an individual's acceptance of technology by measuring their intentions. The study found that the public was more likely to accept UAM services offered by well-known companies. Meanwhile, Anania et al. (2018) observed significantly higher support for neighborhood drone operations among African American residents compared to White residents.

Regarding service supply characteristics, safety, reliability, and user control rights are the most critical influencing factors. Merat et al. (2017) emphasized that system reliability and safety constitute the foundation for

building trust.

External environmental conditions, including weather, infrastructure development, policies and regulations, competitive pressure from alternative transport modes, community acceptance, etc. (Vascik, 2017, Zhuo et al., 2025) significantly impact UAM development. A NASA survey (Goyal et al., 2018) revealed that up to 81% of respondents were willing to use UAM services in both hot and cold weather. However, worsening weather conditions (e.g., snowfall, fog, or turbulence) substantially increased users' safety concerns. In addition, regional disparities in airspace management policies directly constrain UAM deployment.

Based on a quantitative analysis of travel mode choice influencing factors, potential user groups of the UAM system and their spatial distribution characteristics can be accurately identified. These demand-side analytical results provide significant guidance for vertiport location selection decisions. An in-depth understanding of the spatial distribution pattern and dynamic change characteristics of UAM demand is an important prerequisite and theoretical foundation for scientifically planning the vertiport network.

### 2.2 UAM demand estimation

Studies on UAM demand estimation can be categorized into micro-level and macro-level analyses based on the granularity of investigation. Microlevel estimation focuses on individual travel decisions, while macro-level estimation deals with group aggregation characteristics.

In the field of the micro-level estimation, scholars have developed various innovative modeling approaches. Roy et al. (2021) constructed a mode choice model based on discrete choice theory, which can accurately identify high-potential users for business airport shuttle services by analyzing travelers' utility functions. Wu and Zhang (2021) proposed an integer programming-based optimization model that innovatively incorporates the time-value function of travelers in the Tampa Bay area (Florida) to estimate demand through travel cost minimization.

In the field of the macro-level estimation, Becker et al.'s (2018) gravitational model study represents a groundbreaking contribution. Their model enhances the traditional distance decay function by incorporating innovative indicators such as urban economic scale and industrial complementarity, successfully predicting intercity

**Table 1** Key demand factors for UAM adoption

Key demand factors	Characteristics and elements
Individual user characteristics	Subjective characteristics: Public acceptance of UAM, travel preferences, brand awareness, etc. Objective characteristics: Age, gender, purchasing power, political orientation, nationality, etc.
Service supply characteristics	Comfort, reliability, safety, cost-effectiveness, and flexibility
External environmental conditions	Weather conditions, infrastructure development, policy and regulations, incentives from alternative transport modes, and community acceptance

UAM demand patterns for major global urban agglomerations by 2042. Furthermore, research from professional consulting institutions has expanded the scope of application scenarios.

Research on UAM demand estimation can be categorized into two service types: air taxi services and airport shuttle services, as summarized in Table 2.

In terms of the demand estimation for air taxis, Ilahi et al. (2021) constructed the first large-scale discrete choice model covering an entire metropolitan area, systematically evaluating indicators of willingness to pay, including the value of travel time, and the cross-elasticity of various transportation modes. Meanwhile, Rimjha et al.'s (2021) empirical analysis for Northern California further shows that fare levels are decisive for UAM demand, and that sufficient market size can only be developed in the lower fare range.

In terms of the demand estimation for the UAM airport shuttle service, scholars have explored key issues such as user preferences, pricing strategies and economic feasibility through discrete choice models and empirical analyses. Brunelli et al. (2023) identified the main factors influencing users' choices of UAM airport shuttles for Bologna Airport in Italy: income level, air travel frequency and willingness to carpool positively impact demand, while habits of relying on ground transportation, high household car ownership, and lack of experience with automated driving systems negatively affect demand. Hae Choi and Park (2022) quantified competitive fares for UAM through a multinomial logit model based on ground transportation data from Incheon Airport in Republic of Korea. They pointed out that relying solely on time-saving advantages is difficult to achieve

economic feasibility and should be supplemented by dynamic pricing and operator collaboration strategies.

In research exploring UAM as a component of hybrid transportation services, scholars have focused on factors influencing user acceptance and its potential environmental benefits. Al Haddad et al. (2020) found that UAM acceptance is significantly influenced by trust in automation, perceived value of time, and social attitudes through factor analysis and ordered logit modeling. Cho and Kim (2022), based on a case study of Seoul, demonstrated that UAM has significant emission-reduction potential for medium-distance travel.

## 2.3 Vertiport location optimization

### 2.3.1 Clustering algorithms

The application of the *K*-means clustering algorithm in vertiport location optimization is primarily reflected in its ability to identify potential vertiport locations through spatial data clustering analysis. This method can effectively analyze the spatial distribution patterns of traffic demand. Specifically, the algorithm aggregates high-demand-density traffic analysis zones or population activity hotspots into distinct demand clusters. The travel demand within each cluster can then be served by its corresponding cluster center (i.e., the candidate vertiport locations). This approach optimizes both the spatial coverage and demand allocation efficiency of vertiports, thereby providing data-driven decision support for urban air traffic network planning. By dividing a city into regions and grouping similar regions into categories, planners can better understand the demand characteristics and variations across different areas.

**Table 2** Key UAM demand studies by service type

Service type	Year	Continent	Country /region	City	Data type (Sample size)	Modeling approach	Source
Air taxi	2018	Asia	Indonesia	Greater Jakarta	RP/SP (5,143)	Multinomial & Mixed Logit Models	Ilahi et al. (2018)
Air taxi	2017	Global	–	–	SP (692)	Correlated Grouped Random Parameter Model	Ahmed et al.
Air taxi	2018	North America	USA (multi-state)	Atlanta, Boston, Dallas-Fort, Worth, San Francisco, Los Angeles	SP (2,500)	Multinomial, Logit, Mixed, Logit & Latent Class Models	Boddupalli et al.
Air taxi	2018	Europe	Germany	Munich	SP (228)	Multinomial & Mixed Logit Models	Fu et al.
Air taxi	2019	North America	USA (California)	Northern California Urban Area	Multi-source Data set	Mixed Logit Model	Rimjha et al.
Airport shuttle	2022	Europe	Italy	Bologna	SP (225)	Multinomial & Mixed Logit Models	Brunelli et al.
Airport shuttle	2019	Asia	Republic of Korea	Seoul	Airport Ground Access Data set	Multinomial & Mixed Logit Models	Hae Choi & Park
Airport shuttle	2019	North America	USA (California)	Los Angeles	Multi-source Data set	Mixed Logit Model	Rimjha et al.
Mixed services	2018	Europe	Germany	Munich	SP (221)	Exploratory Factor Analysis, Multinomial Logit & Ordered Logit Models	Al Haddad et al.
Mixed services	2020	Asia	Republic of Korea	Seoul	SP (1,710)	Multinomial & Mixed Logit Models	Cho & Kim

The *K*-means algorithm and the *K*-means++ algorithm are widely used in current vertiport location planning problems (Arthur and Vassilvitskii, 2006; Jiang et al., 2025; Zhou et al., 2025a). Rajendran and Zack (2019) proposed an improved method to enhance the initial seed selection in *k*-means. First, they calculated the fitness of candidate locations based on the percentage of demand satisfaction, then selected the top 10 candidate locations as inputs to the *k*-means algorithm. Compared to traditional *k*-means, this approach generates significantly fewer clusters, thereby limiting the number of required vertiport locations and improving operational efficiency. Wei et al. (2020) applied the *K*-means++ algorithm to initialize both continuous and discrete *p*-median models by minimizing the demand-weighted distance from customers to UAM infrastructure. Their study highlights the importance of optimizing infrastructure locations to ensure efficient capital utilization.

There are many other innovative combinations based on the *k*-means clustering algorithm. For example, the multi-criteria initiation algorithm integrates multi-criteria decision-making with an iterative *k*-means clustering process to construct a two-phase location planning model. This model explicitly incorporates socio-economic factors of potential UAM passengers (Salama and Srinivas, 2020; Zhou et al., 2025b). The *k*-median algorithm, a hierarchical clustering method, can partition geographic areas into regions and further group passengers into demand-based clusters. Lim and Hwang (2019) applied the *k*-median algorithm to cluster transportation zones in Seoul and employed the Silhouette method (Rousseeuw, 1987) to validate cluster quality.

### 2.3.2 Other methods

Rath and Chow (2022) developed a demand model integrating travelers' decision-making processes and UAM service choices, proposing a generalized optimization framework based on the hub location problem to optimize vertiport placement in urban areas. Chen et al. (2022) introduced a grid-discretization-based location selection model that screens candidate locations by relaxing grid constraints and innovatively employs a variable neighborhood search algorithm to solve the mathematical programming problem. Other scholars have extended classical operations research frameworks to address this challenge. For instance, Ale-Ahmad and Mahmassani (2021) formulated the location selection problem as a capacitated location-allocation-path problem with time windows, establishing a mixed-integer programming model to derive optimal solutions.

### 2.4 Research gaps and contributions

Compared with existing research, the innovation of this paper mainly lies in the systematic integration of the

methodology and the dynamic and scenario-driven optimization framework.

First, in terms of methodology, this study does not regard UAM demand forecasting and facility site selection as two independent links. Instead, it constructs an integrated analytical framework that organically connects the binary Logit selection model based on RP/SP surveys, potential user identification based on time value coefficients, *K*-means spatial clustering, and multi-objective integer programming. This framework effectively bridges the gap between the behavior of micro individuals and the planning of macro networks.

Secondly, in terms of model architecture, addressing the limitation where most existing site selection models are static optimizations, this paper innovatively proposes a three-stage multi-objective integer programming (TP-MOIP) model. The core advantage of this model lies in its "phased" optimization mechanism, which can simulate the phased construction process of the vertiport network and provide decision-makers with a clear, phased development roadmap that considers efficiency at each stage. This represents a significant advance over traditional single-stage static models.

Finally, at the data and application level, this study combines RP/SP surveys and introduces a time value coefficient to accurately identify "time-sensitive users" as the core target customer group. This approach is more nuanced and precise than discussing "potential users" in general terms. Through an in-depth sensitivity analysis of the Shenzhen case, the dynamic impact patterns of key parameters such as land cost on planning schemes were revealed, providing a valuable regional complement and empirical validation to the existing research system primarily based on European and American cities.

## 3 Travel choice modeling

### 3.1 Questionnaire survey

In the field of travel behavior research, the primary methods for studying individuals' mode choice include RP and SP surveys.

RP surveys rely on actual behavioral data, assuming that individual choices reflect true preferences and utility maximization. Their key strength lies in data objectivity and authenticity, but estimation bias may occur due to constrained choice sets in real-world scenarios. To address this issue, researchers employ methods such as conditional logit models and mixed logit models to mitigate choice-set limitations. SP surveys, on the other hand, collect preference data through hypothetical scenarios. While their flexible experimental design is advantageous, they are prone to social desirability bias and hypothetical bias. Techniques like conjoint analysis and discrete choice experiments (DCEs) are commonly used to mini-

mize these biases. Both RP and SP methods have complementary strengths and limitations: RP provides real-world validity but suffers from limited choice variability, whereas SP offers design flexibility but may lack behavioral realism. To enhance the robustness of findings, this study integrates RP and SP data, enabling a more comprehensive analysis of travel mode choices and improving the reliability of preference inferences.

The RP survey in this study comprises 14 questions, including 8 on travel characteristics and 6 on socio-economic attributes. Travel characteristics focused on respondents' most recent or typical intercity trip. Key behavioral data (e.g., trip purpose, chosen mode, and one-way cost) were collected through structured questions to minimize recall bias. Socio-economic variables covered gender, age, occupation, and income. Sensitive information (e.g., income and job position) was grouped into intervals (e.g., low/medium/ high tiers) to balance privacy concerns with analytical needs. These variables are complementary: Travel parameters (distance, cost, etc.) directly capture behavioral preferences, while socio-economic factors explain group variations (e.g., high-income individuals preferring faster/more expensive modes, and car owners favoring driving). This multidimensional approach provides robust variable inputs for multinomial logit models, enabling precise estimation of factor weights. It is worth noting that although the intervalization of sensitive information loses some data accuracy, it meets the privacy protection needs of Chinese respondents and significantly improves the questionnaire completion rate.

The SP survey in this study comprises seven core questions designed to systematically assess willingness to use air mobility services. For travel intention measurement, a 1–7 point scale was employed to evaluate both regular and peak-hour mode choice preferences (scores 5–7 coded as 1 for “would choose”; 1–4 coded as 0 for “would not choose”), preserving response gradients while accommodating binary choice modeling. Willingness to pay was assessed through dual approaches: open-ended monetary value questions combined with travel-cost multiples, capturing both absolute price sensitivity and income-adjusted preferences. Connection service evaluation incorporated: time (< 5 min = 0; 5–10 min = 1; > 10 min = 2) and distance (< 3 km = 0; 3–5 km = 1; > 5 km = 2), as well as the open-ended questions of the connection mode, providing a basis for service optimization. This multidimensional design ensures data robustness while meeting analytical requirements for discrete choice modeling.

AAM-enabled tourism is emerging as a significant sector within the tourism and transportation industries, particularly appealing to high-net-worth individuals and quality-seeking tourists. 2024 market data indicates an average spending per customer ranging from 2,000 to 5,000 CNY in this sector, underscoring its premium

market positioning. This study surveyed Executive Master of Business Administration (EMBA) and Master of Business Administration (MBA) students at Sun Yat-sen University and other high-income groups, distributing 9,000 questionnaires with 1,386 valid responses collected. With a 95% confidence level and a margin of error within 6%, the results demonstrate high statistical validity, providing reliable data for further analysis. The classification of the questionnaire survey questions is shown in Table 3.

To systematically analyze individual travel choice behavior, the information in the questionnaire were categorized into four groups: personal attributes, family attributes, travel attributes, and other attributes. Figure 2 displays the proportional distribution of these categories, providing a visual representation of the data structure for subsequent analysis.

As shown in Fig. 2, the survey results indicate a relatively balanced gender distribution. The majority of respondents are young to middle-aged individuals from middle-income groups, with most holding grassroots or middle-level positions. In terms of car preference, economy cars are the most popular. Regarding family car ownership, nearly 70% of families own one car, while the proportion of families without cars is similar to those with two cars; families with multiple cars account for a small proportion. For family size, three-to-four-member households are the most common, followed by households with five or more members. Travel purposes include commuting, tourism, business trips, and visiting relatives and friends. For travel scenarios, cross-city travel is the most common, followed by trips to city centers and transportation hubs. Usage of public transportation and private transportation is roughly equal. Regarding travel companions, solo and paired trips are the most frequent, and self-funded travel is significantly more common than employer-funded travel. Additionally, most respondents are willing to pay additional fees under specific conditions. For transfer time and distance, respondents generally prefer shorter durations and distances.

In the process of data analysis, the Multinomial Logit Model (MNL) was adopted. This model is a type of discrete selection model and is widely used to analyze the selection behavior of individuals in a finite selection set. In the context of UAM travel choices, the MNL model can effectively reveal the competitive relationship among different travel modes and predict the probability of an individual choosing a specific travel mode. The basic formulation of the MNL model is as follows:

$$P_{ij} = \frac{e^{V_{ij}}}{\sum_{k \in C} e^{V_{ik}}}, \quad (1)$$

where  $P_{ij}$  represents the probability of individual  $i$  choosing transportation mode  $f$ , and  $V_{ij}$  denotes the utility

**Table 3** Classification of survey questions

Category	Question description	Summary
RP survey	Q1. Primary purpose of the above trip	Trip purpose
	Q2. Estimated one-way distance of the above trip (km)	Distance
	Q3. Transportation mode actually used for the above trip	Mode choice
	Q4. Frequency of congestion during the above trip	Congestion level
	Q5. Typical one-way travel time for the above trip (min)	Travel time
	Q6. Number of accompanying persons during the trip	Group size
	Q7. One-way cost of the above trip	Cost
	Q8. Primary funding source for the trip expenses	Cost source
	Q9. User type	User type
	Q10. Gender	Gender
	Q11. Age	Age
	Q12. Annual personal income before tax	Income
	Q13. Current job position	Occupation
	Q14. Number of family members	Household size
	Q15. Number of cars owned by household	Car ownership
SP survey	Q16. Willingness to use UAM in future trips	UAM adoption
	Q17. Willingness to use UAM during peak congestion hours	Peak-hour UAM choice
	Q18. Maximum acceptable one-way fare for UAM on the above trip	Absolute WTP
	Q19. If UAM reduces travel time to 1/4 of current duration (with safety guaranteed), acceptable fare premium over current mode (times)	Relative WTP
	Q20. Maximum acceptable first/last-mile connection time (minutes)	Transfer time
	Q21. Maximum acceptable first/last-mile connection distance (km)	Transfer distance
	Q22. Preferred first/last-mile connection mode	Transfer mode

function of mode  $j$  with  $C$  being the set of all available transportation alternatives. In this study, there are only two transportation options available: choosing UAM or not choosing UAM. Therefore, the MNL model can be simplified to a Binary Logit Model (BLM). The basic formulation of the model can be expressed as:

$$P(Y = 1 | X) = \frac{e^{V(X)}}{1 + e^{V(X)}}, \quad (2)$$

where  $P(Y = 1 | X)$  denotes the probability of choosing UAM given attributes  $X$ ,  $V(X)$  represents the utility function typically specified as  $V(X) = \beta_0 + \beta_1 X_1 + \beta_2 X_2 + \dots + \beta_n X_n$ , with  $\beta$  being the parameter vector and  $X$  the attribute vector.

The model parameters are estimated via maximum likelihood estimation (MLE). The coefficients directly indicate the directional effects of attributes on UAM adoption probability: negative values correspond to decreased preference, while positive values suggest increased preference. These quantitative results inform policy formulation and marketing strategies.

The final results indicate an average UAM adoption probability of 0.167, suggesting that 16.7% of observed individuals exhibit a preference for UAM. While this

proportion remains modest, it demonstrates measurable market potential for this emerging transportation mode, providing a promising development signal.

### 3.2 Numerical calculation of the time value coefficient

Time cost is a critical factor in travel mode choice. This study employs the time value coefficient, quantified by individuals' willingness-to-pay for time savings, to reflect subjective time valuation. The time value coefficient directly influences transportation mode selection, enabling identification of UAM service's potential adopters.

Specifically, the calculation formula for the time value coefficient is as follows:

$$v = \frac{C_{\text{Taxi}} - C_{\text{UAM}}}{T_{\text{UAM}} - T_{\text{Taxi}}}, \quad (3)$$

where  $C_{\text{Taxi}}$  and  $C_{\text{UAM}}$  denote the price costs of taxi and UAM, respectively, while  $T_{\text{Taxi}}$  and  $T_{\text{UAM}}$  represent their corresponding travel times.

This study assumes  $T_{\text{Taxi}} = k \cdot T_{\text{UAM}}$ , where  $k$  is a constant. Here,  $T_{\text{Taxi}}$  is the observed taxi travel time, whereas  $T_{\text{UAM}}$  is derived by dividing the straight-line

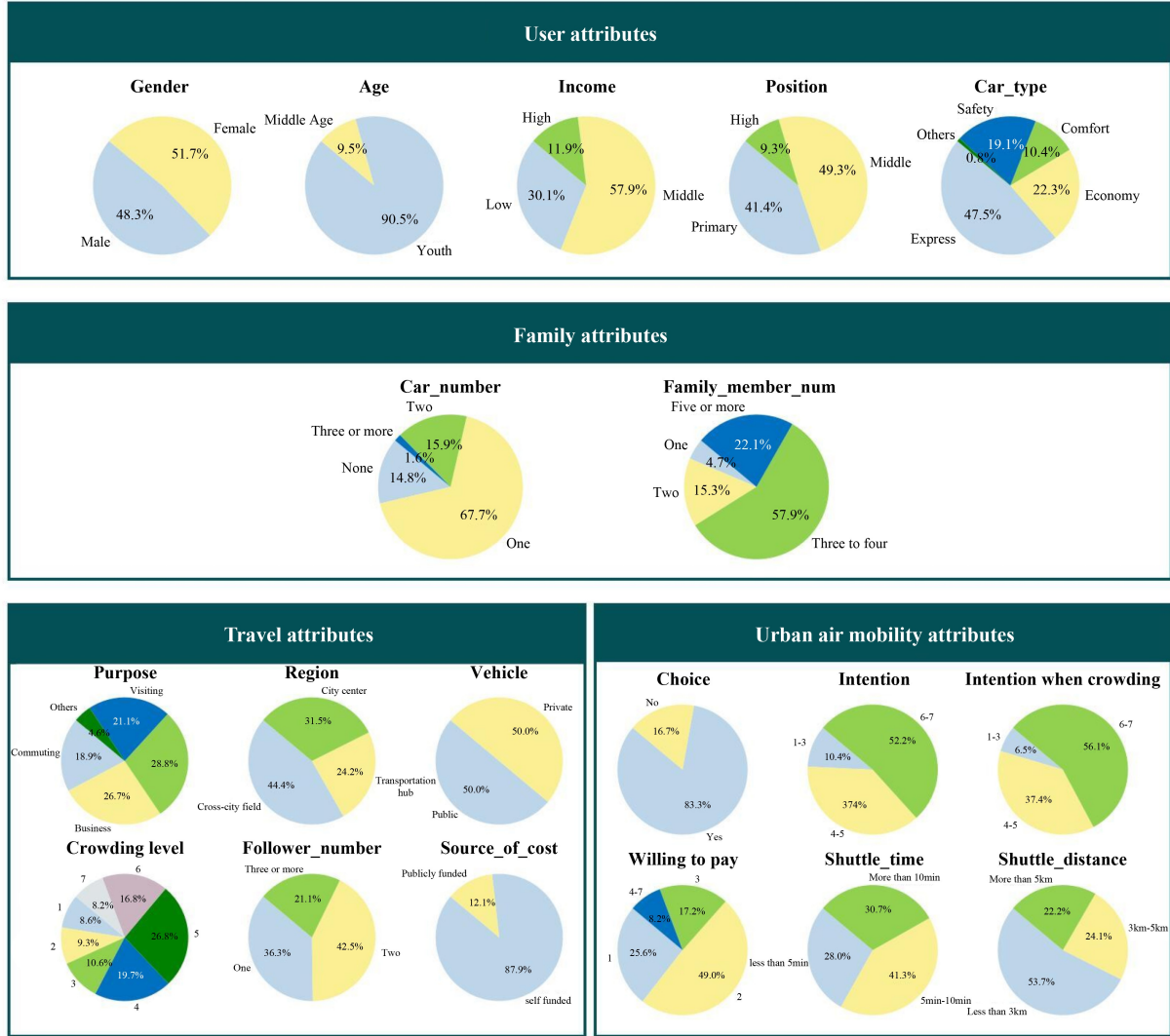


Fig. 2 Descriptive proportional structure diagram of the questionnaire.

distance between origin and destination by the cruising speed. This assumption aligns with empirical observations and prior research on taxi-UAM travel time ratios. The value  $k = 5$  is adopted based on De-loitte's report (2022), where electric vertical landing and takeoff (eVTOL) demonstrate 5 times higher cruising speeds than ground transportation. For a 27-mile commute, ground transit requires 74 minutes versus eVTOL's 10-min cruise time (25 miles). Including takeoff/landing and safety checks, the total eVTOL time reaches 29 minutes. The time efficiency becomes more pronounced for longer distances. Notably, during the first cross-bay demonstration flight on February 27, 2024, AutoFlight's eVTOL completed the Shenzhen Shekou-Zhuhai Jiuzhou route in 20 minutes, achieving 9× time reduction compared to the 2.5-3 hours needed by ground transport.

Based on the Box-Cox transformation principle in statistical modeling, this study applies a power transformation to individual time value coefficient, effectively

improving the distributional properties of the raw data. The Box-Cox transformation constructs a continuously differentiable family of power transformations through parameter  $\lambda$ , with the mathematical expression given by:

$$y(\lambda) = \begin{cases} \frac{y^\lambda - 1}{\lambda}, & \text{if } \lambda \neq 0 \\ \ln(y), & \text{if } \lambda = 0. \end{cases} \quad (4)$$

The transformation optimizes parameter  $\lambda$  through maximum likelihood estimation, ensuring the transformed data  $y(\lambda)$  satisfies normality assumptions. When  $\lambda = 1$ , it reduces to a linear transformation; when  $\lambda = 0$ , it becomes logarithmic; other values enable nonlinear scaling. For better data presentation, we additionally apply linear shifting. Through this parametric variance-stabilizing approach, the originally right-skewed time value coefficients are transformed into approximately normal distributions, as shown in Figure 3. Based on the statistical properties of the transformed data, this study identifies

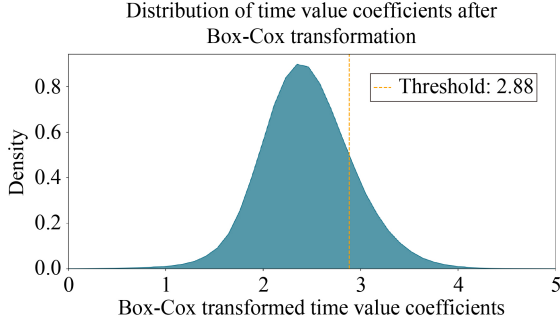


Fig. 3 Normality transformation results.

individuals with time value coefficients in the top 16.7th percentile as the time-sensitive cohort. This subgroup exhibits significantly higher marginal utility of time and greater propensity for mode switching given UAM’s time-saving advantages, providing critical inputs for target market segmentation in UAM demand modeling. These analysis results can provide data support for the location optimization of vertiport and optimize the accessibility and convenience of UAM services based on the spatial distribution characteristics of demand.

## 4 Methodology for vertiport location optimization

In UAM system planning, vertiport location critically impacts operational efficiency and service quality. This study adopts a multi-phase location selection optimization method based on spatial clustering, comprehensively considering the urban spatial structure, the distribution of travel demands and resource constraints, and constructs a complete decision support framework for vertiport location Optimization.

### 4.1 K-means clustering

In vertiport placement, identifying optimal locations is critical. To address this challenge, this study employs the K-means clustering algorithm to analyze OD (Origin-Destination) points and determine potential verti-port locations. The selection of K-means over alternative methods such as hierarchical clustering, K-medoids, and DBSCAN is based on several key considerations:

1) Scalability and efficiency: Compared to hierarchical clustering with high computational complexity or K-medoids algorithms with higher computational costs, the K-means algorithm demonstrates significant efficiency advantages when processing the large-scale online car-hailing order data in this study (328,716 valid records), which is crucial for iterative model development and scenario testing.

2) Fitness for centroid-based site selection: Unlike density-based methods such as DBSCAN, K-means is a

centroid-based clustering method. This characteristic makes it particularly suitable for facility location problems, as the generated cluster centroids can naturally serve as candidate vertiport locations and minimize the total travel distance (or cost) of passengers within clusters, which aligns with the core objective of location problems.

3) Alignment with policy objectives: This study requires setting explicit vertiport construction quantity targets based on policy. The characteristic of K-means requiring pre-specification of the  $k$  value perfectly aligns with this policy planning requirement, providing a clear, deterministic, and policy-compliant network planning framework. In contrast, methods like DBSCAN determine the number of clusters based on data density, which may not meet established infrastructure targets.

The K-means algorithm partitions data into  $k$  clusters by minimizing the mean squared Euclidean distance between points and cluster centers, where each center is the arithmetic mean of its constituent points, expressed mathematically as:

$$\mu_i = \frac{1}{|S_i|} \sum_{x \in S_i} x, \quad (5)$$

where  $S_i$  represents the set of data points in the  $i$ -th cluster,  $\mu_i$  is the centroid of the  $i$ -th cluster,  $x$  denotes a data point, and  $|S_i|$  indicates the number of data points in cluster  $S_i$ . The centroid characterizes the data in its cluster, with the Residual Sum of Squares (RSS) serving as the metric - the sum of squared distances between each vector and its centroid across all vectors, expressed as:

$$\text{RSS} = \sum_{i=1}^k \sum_{x \in S_i} \|x - \mu_i\|^2. \quad (6)$$

The goal of the k-means algorithm is to minimize the RSS, which is formulated as:

$$\min_{\mu_1, \mu_2, \dots, \mu_k} \sum_{i=1}^k \sum_{x \in S_i} \|x - \mu_i\|^2. \quad (7)$$

The K-means algorithm requires pre-specifying the parameter  $k$ , then iteratively repeats the clustering process until the cluster centers’ positions stabilize. Specifically, it first randomly selects  $k$  data points as initial cluster centers; then assigns each data point to its nearest cluster center, forming  $k$  clusters; subsequently recalculates each cluster’s centroid; and finally repeats the assignment and update steps until either the cluster centers converge or the preset maximum iterations are reached. Based on Shenzhen’s relevant policy documents, this study sets  $k = 200$ .

To evaluate the k-means clustering quality, two metrics are employed: the Silhouette Coefficient and Davies-Bouldin Index (DBI). The Silhouette Coefficient ranges

from  $-1$  to  $1$ , where values closer to  $1$  indicate better clustering performance. Its calculation formula is as follows:

$$s(i) = \frac{b(i) - a(i)}{\max\{a(i), b(i)\}}, \quad (8)$$

where  $a(i)$  represents the average distance from data point  $i$  to all other points within the same cluster, while  $b(i)$  denotes the average distance from data point  $i$  to all points in the nearest neighboring cluster. The mean value of the Silhouette Coefficient across all data points reflects the overall clustering quality of the entire dataset.

The DBI is calculated as follows:

$$\text{DBI} = \frac{1}{k} \sum_{i=1}^k \max_{j \neq i} \left( \frac{\sigma_i + \sigma_j}{d(c_i, c_j)} \right), \quad (9)$$

where  $\sigma_j$  denotes the average distance between data points and the centroid within cluster  $i$ , and  $d(c_i, c_j)$  represents the distance between the centroids of clusters  $i$  and  $j$ .

In this study, the k-means algorithm was applied to perform spatial clustering analysis on Shenzhen's online car-hailing order data. The number of clusters was set to  $k = 200$ , a parameter determined primarily by the construction target of 174 vertical take-off and landing airports outlined in the Shenzhen High-Quality Construction Plan for Low-Altitude Infrastructure (2024–2026) (Development and Reform Commission of Shenzhen Municipality, 2024), with adjustments made based on regional area and service radius. The data source comprised 328,716 valid order records from the On Time platform in March 2024, after excluding short-distance trips ( $< 5$  km) and invalid orders during preprocessing.

The clustering quality evaluation yielded a silhouette coefficient of  $0.43$  and a DBI of  $0.77$ , indicating strong intra-cluster homogeneity and inter-cluster separation, thus meeting the research requirements.

## 4.2 Tri-phase multi-objective integer programming model

This study addresses the location selection problem for UAM vertical take-off and landing fields and constructs a three-phase multi-objective integer programming model (TP-MOIP) based on cluster analysis. The model adopts an normalized weighted synthesis method, which transforms the dual-objective optimization problem of maximizing demand coverage and minimizing operating costs into a single objective function through normalization and weight allocation mechanisms, achieving multi-objective collaborative optimization while maintaining computational efficiency.

The TP-MOIP model innovatively establishes a spatio-temporal collaborative optimization framework: In the

temporal dimension, the construction period is divided into three consecutive phases with clear engineering significance. By introducing phase variables to reflect the dynamic decision-making process of UAM network construction, the model prioritizes high-demand areas in the initial phase and gradually improves cost-effectiveness in later phases, avoiding excessive investment while ensuring rapid network formation. In the spatial dimension, a refined coverage assessment system is established based on demand distribution patterns. The two dimensions are organically integrated through the following constraints:

1) Construction phase constraints ensure that investment scales match implementation capacity at each phase;

2) Demand coverage constraints guarantee progressive improvement in spatial service capacity;

3) Budget allocation constraints optimize the spatio-temporal distribution of construction funds.

This framework effectively resolves the temporal discontinuity and spatial incoordination of traditional planning models.

### 4.2.1 Assumptions

The multi-objective integer programming model established in this study is based on the following fundamental assumptions:

1) The construction cost of vertiports is positively correlated with the housing price level in their respective traffic analysis zones.

2) The human resource cost for vertiport operations can be effectively characterized by the average wage level of their respective regions.

3) The Euclidean distance from vertiports to the city center can effectively reflect their transportation accessibility.

4) The spatial distribution pattern of ride-hailing origin-destination (OD) data can effectively represent potential UAM demand.

5) The Voronoi polygon boundaries formed by k-means clustering define service coverage areas, with each cluster's travel demand requiring service exclusively from its centroid vertiport, prohibiting cross-cluster demand allocation.

### 4.2.2 Notation and mathematical formulation

The following notation is used in the formulation of the TP-MOIP. Let  $\mathcal{J} = 1, 2, 3$  denote the set of construction phases and  $\mathcal{J}$  represent the complete set of candidate vertiports. For each vertiport  $j \in \mathcal{J}$ , we define  $f_j$  (in meters) as its transportation accessibility,  $p_j$  as its demand coverage capacity,  $r_j$  (in CNY) as its rental cost, and  $s_j$  (in CNY) as its salary expenditure. At the system level,  $P_{\text{total}}$  denotes the total demand requirement,  $R_{\text{total}}$

represents the total rental budget (in CNY), and  $S_{\text{total}}$  indicates the total salary expenditure budget (in CNY). The weighting coefficients  $\alpha$ ,  $\beta$ , and  $\gamma$  satisfy the constraint  $\alpha + \beta + \gamma = 1$ . For each construction phase  $j \in \mathcal{J}$ ,  $N_i$  constrains the maximum number of vertiports that can be established,  $R_i$  represents the allocated site construction budget (in CNY),  $S_i$  indicates the salary expenditure budget (in CNY), and  $F_i$  specifies the transportation accessibility requirement (in meters) that must be achieved.

With the parameter notation defined, we now introduce the decision variables. Let  $\delta_{ij} \in 0,1$  equal one if vertiport  $j$  is established in phase  $i$ .

Based on these definitions, we formulate the TP-MOIP model, which employs an innovative weighted comprehensive optimization approach to simultaneously address two competing key objectives: maximizing demand coverage and minimizing construction costs. To overcome the technical challenge of comparing differently-scaled indicators, the model introduces an enhanced bipolar normalization technique for handling multi-objective dimensional disparities. The resulting normalized bi-objective function is mathematically expressed as follows:

$$\begin{aligned} \max Z = & \alpha \cdot \left( \sum_{i \in I} \sum_{j \in J} \delta_{ij} \frac{p_j}{P_{\text{total}}} \right) - \beta \cdot \left( \sum_{i \in I} \sum_{j \in J} \delta_{ij} \frac{r_j}{R_{\text{total}}} \right) \\ & - \gamma \cdot \left( \sum_{i \in I} \sum_{j \in J} \delta_{ij} \frac{s_j}{S_{\text{total}}} \right). \end{aligned} \quad (10)$$

For the UAM location selection problem, accounting for the complexity of actual construction and the necessity of phased development, this study extends a multi-objective integer programming model by introducing phase-specific constraint conditions. Specifically, the model aims to gradually deploy UAM locations across multiple construction phases to simultaneously maximize total demand coverage and minimize total expenditure, while satisfying budget allocation, salary expenditure, and transportation accessibility constraints at each phase. Specifically, the model incorporates the following constraints:

$$\sum_{i \in I} \delta_{ij} \leq 1, \forall j \in J. \quad (11)$$

1) Vertiport quantity constraint: This constraint limits the number of vertiports  $N_i$  that can be constructed in each phase  $i$  to comply with resource and budget limitations. By rationally controlling the construction scale at each phase, it effectively manages resource allocation and ensures sustainable project development.

$$\sum_{j \in J} \delta_{ij} \leq N_i, \forall i \in I. \quad (12)$$

2) Land cost constraint: This ensures the land cost in each phase  $i$  does not exceed the budget  $R_i$ . As land cost constitutes a major component of vertiport construction, controlling it helps reduce overall investment risks and enhances project feasibility:

$$\sum_{j \in J} r_j \delta_{ij} \leq R_i, \forall i \in I. \quad (13)$$

3) Salary expenditure constraint: This guarantees the salary expenditure in each phase  $i$  remains within budget  $S_i$ . Being a crucial part of operational costs, proper salary control ensures operational sustain-ability:

$$\sum_{j \in J} s_j \delta_{ij} \leq S_i, \forall i \in I. \quad (14)$$

4) Transportation accessibility constraint: This requires the transportation accessibility metric  $f_j$  of vertiports in each phase  $i$  to meet the minimum threshold  $F$ , ensuring convenient access. Maintaining adequate accessibility improves UAM service convenience and user satisfaction:

$$\sum_{j \in J} f_j \delta_{ij} \geq F_i, \forall i \in I. \quad (15)$$

## 5 Case study

### 5.1 Data description

The key data used for model construction are obtained from online channels and undergoes strict data cleaning and preprocessing procedures.

The housing price data in this study primarily comes from Lianjia's website. Using Python web crawler technology, we collected real-time housing price information for residential communities across all 10 administrative districts of Shenzhen, resulting in a total of 4,232 valid data points. The spatial distribution and statistical characteristics of these housing prices are visualized in Fig. 4.

Human resource cost data was estimated based on comprehensive queries of relevant web page information, combined with industry standards and market research data.

Transportation accessibility, as an important indicator of regional transportation convenience, was quantified by calculating the Euclidean distances from each vertiport to Shenzhen's city center. Using high-precision map data, we precisely measured these distances to serve as quantitative indicators of traffic accessibility.

To clearly present the distribution characteristics of the key input variables, Table 4 summarizes the descriptive statistics (including mean, standard deviation, minimum,

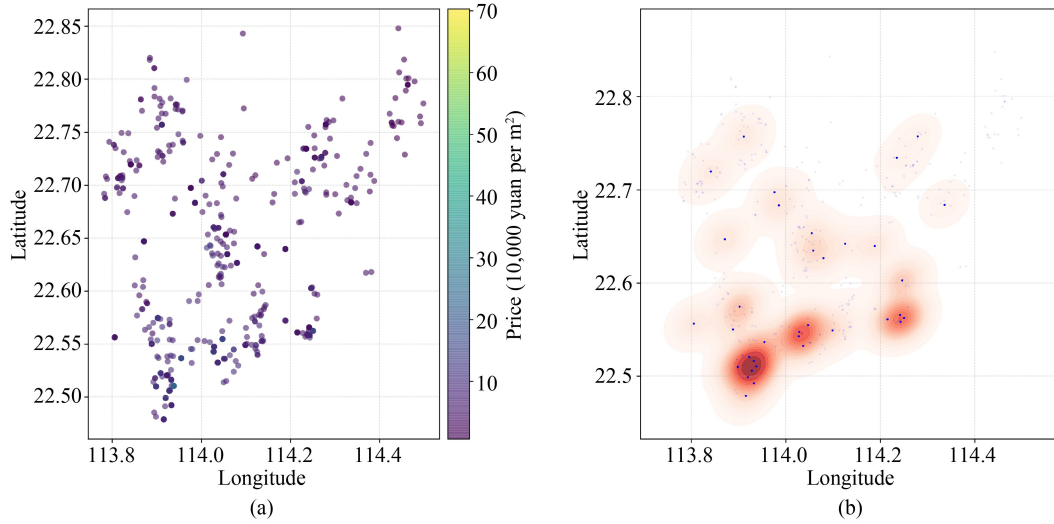


**Fig. 4** Visual analysis of housing prices in Shenzhen for (a) Geographical distribution of housing prices and (b) Density heat map of housing prices (Data source: Lianjia website).

**Table 4** Descriptive statistics of key variables

Variable	Mean	Std. Dev.	Min	Max	Median
Housing price	58,973.38	31,465.93	9,300.00	240,000.00	52,200.00
Human resource cost	14,149.00	2,968.52	9,900.00	20,600.00	13,100.00
Transportation accessibility	8.92	7.37	0.74	33.68	6.31

maximum, etc.) for the three core variables: housing price, human resource cost, and transportation accessibility.

## 5.2 Results

This study employed the Gurobi 9.1.2 optimizer for solution, with a total solution time of 11,806 s. The resulting optimal siting scheme under the TP-MOIP framework exhibits a strategic phased progression: initial construction prioritizes high-demand core areas to ensure immediate service viability, followed by sequential expansion into peripheral regions in the second and third phases. This hierarchical growth pattern effectively balances the immediate maximization of demand coverage with the long-term accommodation of development potential in emerging regions.

Having established the optimal spatial configuration, we now turn to examine the trade-offs inherent in the multi-objective optimization process. We analyze the impact of the weight parameter  $\alpha$  on system performance through a parametric model, using the sum of land and labor costs as the total cost metric. By setting  $\beta = \gamma$  and applying heterogeneous normalization to both demand coverage and cost elements, the Pareto frontier characteristics demonstrate the trade-off between coverage rate and cost objectives. This provides a decision-making framework for resource allocation in UAM network planning. The Pareto analysis diagram is shown in Fig. 5, and

the corresponding numerical results for different  $\alpha$  values are presented in Table 5.

When  $\alpha$  is within the range of 0.65 to 0.9, the model exhibits distinct phased characteristics, reflecting the Pareto frontier properties inherent to multi-objective optimization problems. In this high- $\alpha$  regime, the system maintains a stable high-coverage plateau with fluctuations below 1%, sustaining coverage near 88% while showing limited total cost variation — a hallmark of diminishing marginal returns. This demonstrates that when prioritizing service coverage, the system automatically optimizes resource allocation by selecting location combinations with maximal unit cost coverage efficiency, a configuration robust to minor cost weight adjustments.

When  $\alpha$  is within the range of 0.5 to 0.65, the system undergoes a significant transformation and enters a sensitive transition zone. At this phase, it exhibits a distinct threshold effect. Within this range, the coverage rate begins to show an accelerating downward trend, while the cost-saving effect becomes significantly enhanced. Specifically, for every 0.05 decrease in  $\alpha$ , the average coverage rate drops by approximately 7 percentage points, while achieving about 12% cost savings. This nonlinear response indicates that the system has reached a critical turning point. Beyond this point, continuing to emphasize the cost target will lead to significant sacrifices in coverage quality. A thorough analysis of the solution's structural changes reveals that at this phase, the model begins systematically abandoning locations with higher unit coverage costs that

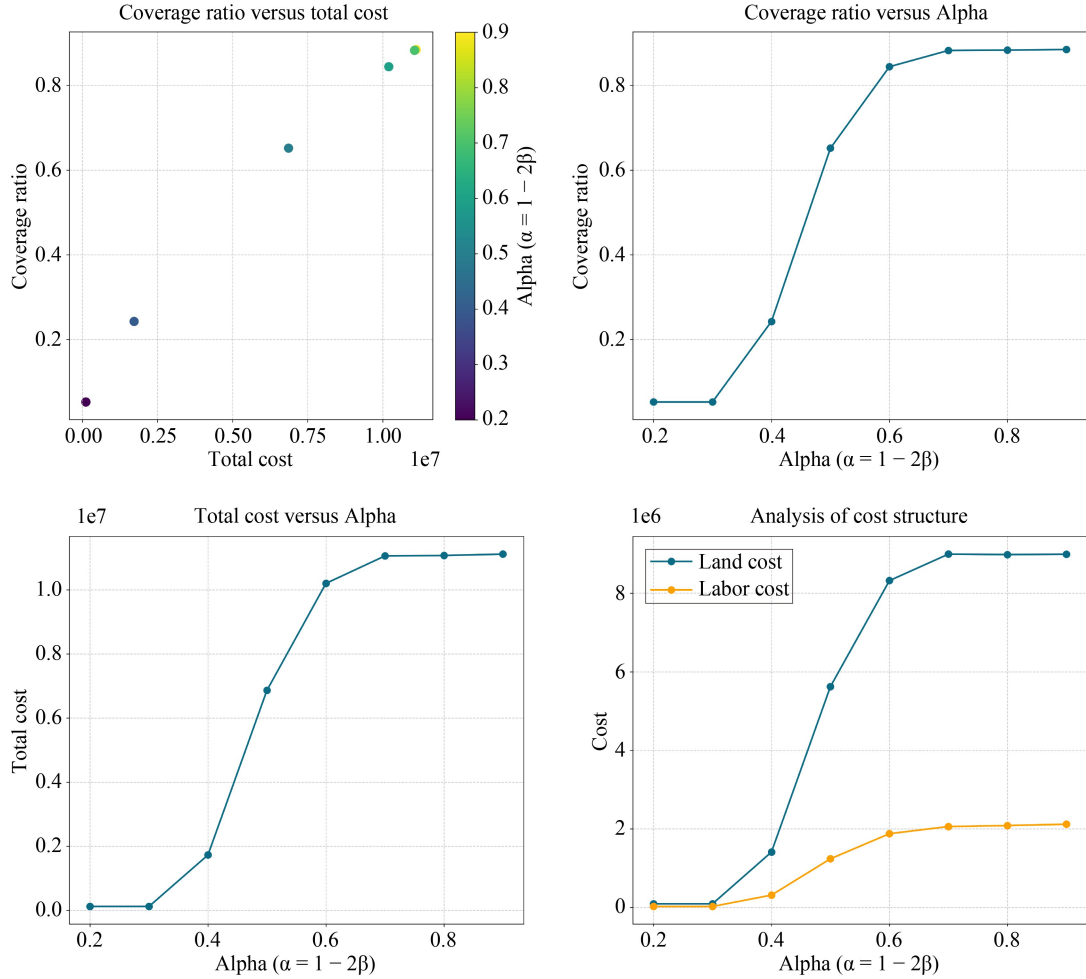


Fig. 5 Pareto analysis results.

Table 5 System performance under different  $\alpha$  values

$\alpha$	Coverage rate (%)	Total cost (10,000 yuan)
0.90	88.42	1109.68
0.80	88.43	1103.57
0.70	88.13	1103.81
0.60	84.13	1013.09
0.50	65.19	686.44
0.40	24.26	172.39
0.30	5.24	11.74
0.20	5.24	11.74

serve key areas, instead selecting alternative solutions with better cost-effectiveness but more limited coverage capabilities. This substitution does not occur uniformly but rather exhibits a typical threshold effect.

When  $\alpha$  is less than 0.5, the system enters the cost-dominated zone. At this point, the rate of decline in coverage further accelerates, showing a nearly linear degradation trend. The most notable feature of this phase is the sharp reduction in the number of locations in

phases two and three, with construction resources highly concentrated in the first phase of the project, leading to a clear “centralization” tendency in the network structure. Although this configuration achieved significant cost savings on paper, it severely weakened the overall service capacity and expansion potential of the network. It is particularly worth noting that when  $\alpha$  is between 0.3 and 0.65, although costs continue to decrease, the coverage loss caused by unit cost savings becomes increasingly significant, reflecting the continuous deterioration of resource allocation efficiency.

From the perspective of spatial allocation, the construction models under different  $\alpha$  values show regular changes. In the region with higher  $\alpha$  values, the resource allocation in the three phases is relatively balanced, and the construction scale of each phase matches the budget proportion well, forming a progressive network expansion path. As  $\alpha$  decreases, the proportion of resource allocation in phase three drops significantly. When  $\alpha$  reaches 0.35, the final construction scale is only about 15% of the total locations, and the budget proportion is less than 9%. Although this “prioritizing the first phase over the later

phases" allocation model controls the total expenditure in the short term, it may lead to insufficient momentum for network development. Specifically, this manifests as insufficient coverage in edge areas and a decline in network connectivity. These hidden costs are often underestimated in simple cost calculations.

From the perspective of the cost structure, the ratio of land cost to labor cost remains relatively stable within the  $\alpha$  value range of 0.65 to 0.9, maintaining a ratio of approximately 4.5:1. This stability indicates that the model automatically maintains a reasonable proportion of operational investment during the optimization process, without extreme cases where a certain type of expenditure is overly compressed in pursuit of cost savings. In the medium  $\alpha$  -value range, the proportion of labor costs increases significantly. This is mainly because in this case, due to the excessive cost weight, costs are severely reduced, the number of operating locations decreases, and the demand coverage rate becomes seriously insufficient.

From the perspective of solution quality and stability,  $\alpha$  performs particularly well in the range of 0.65 to 0.9. The solutions within this range not only achieve a high coverage level, but also exhibit good robustness against parameter disturbances. Tests show that when the cost parameter fluctuates within  $\pm 10\%$ , the location selection structure and spatial distribution of the solution maintain good stability. The computational complexity for the high- $\alpha$  region is significantly higher, with an average of 300 to 850 nodes required to reach convergence, and a computation time of 0.3 to 0.4 seconds. In contrast, for  $\alpha = 0.60$ , the solution requires approximately 50 node explorations and takes 0.06 seconds. This difference stems from changes in the shape of the objective function - which produces more local optimal solutions when coverage is dominant. In particular, when  $\alpha = 0.85$ , the model generated 9 candidate solutions, while for  $\alpha = 0.60$ , only 4 were produced. The diversity of the solution space varies significantly.

The analysis of the weight parameter  $\alpha$  in this section provides clear guidance for trade-off decisions in UAM network planning. The results indicate that the value of  $\alpha$  can be categorized into three critical intervals:

1) When service coverage is prioritized ( $\alpha \in [0.65, 0.9]$ ), the system can achieve efficient operation with approximately 88% coverage while maintaining good robustness, with  $\alpha = 0.8$  recommended as the benchmark value.

2) In the transition interval ( $\alpha \in [0.5, 0.65]$ ), the system exhibits high sensitivity to cost variations, and coverage decreases significantly as  $\alpha$  declines.

3) When  $\alpha < 0.5$ , this range applies to scenarios where cost control is the absolute priority; however, a strictly cost-driven strategy substantially compromises the network's service capability and long-term development potential.

Therefore, decision-makers are advised to select  $\alpha$  directly from the intervals above based on their strategic orientation, considering whether to prioritize service quality or cost control, with  $\alpha = 0.8$  serving as the initial recommended solution for general application scenarios. In practice, the precise calibration of  $\alpha$  can be further refined through structured decision-support frameworks that incorporate stakeholder preferences. For instance, the Analytic Hierarchy Process (AHP) provides a systematic methodology for translating expert evaluations into quantitative weights when trading off multiple conflicting objectives (Thomas and Granberg, 2023). By organizing expert workshops to rank the relative importance of coverage, cost, and other potential factors, planners can derive a context-specific  $\alpha$  value that aligns with local priorities and constraints, thereby enhancing the legitimacy and applicability of the optimization outcomes.

### 5.3 Sensitivity analysis

As an important component of the future smart city transportation system, the location-selection decision of UAM directly affects the operational efficiency and service quality of the entire system. In the actual planning process, decision-makers face the challenges of multiple constraints and uncertainties. This study, by establishing a mathematical optimization model, focuses on examining the influence of three key parameters-land cost budget, labor cost budget, and transportation accessibility indicators-on the demand coverage rate, providing a scientific decision-making basis for the location selection of vertiports.

Sensitivity analysis, as an important tool for evaluating the robustness of mathematical models, can help decision-makers understand the extent to which changes in different parameters affect the system outputs. This study adopted the control variable method to systematically analyze the impact of each parameter varying within a range of  $\pm 20\%$  on the demand coverage across the three phases, revealing the phased characteristics and nonlinear relationships of parameter sensitivity. Additionally, the changes in the number of vertiports in various districts of Shenzhen within the range of parameter variations were explored. The research results not only enrich the theoretical framework of UAM planning but also provide important references for resource allocation and risk management in actual projects.

#### 5.3.1 Land cost budgeting

As shown in Table 6, the impact of changes in land cost budgets on demand coverage shows a significant positive correlation. From Phase 1 to Phase 3, the coverage rate improvement brought about by a 20% increase in the budget was 7.09%, 8.15%, and 13.11% respectively,

**Table 6** Sensitivity analysis of land cost budget

Phase	R1 (-20%)	R2 (-10%)	R3 (Base case)	R4 (+10%)	R5 (+20%)
Phase 1	19.33%	20.51%	16.49%	18.74%	23.58%
Phase 2	45.00%	46.67%	44.73%	50.08%	52.88%
Phase 3	78.16%	83.72%	88.21%	91.24%	91.27%

demonstrating a significant phased amplification effect.

In Phase 1, the increase in budget has a relatively limited impact on the improvement of coverage. This is because the number of initial locations is relatively small, and cost-effective locations are given priority, meaning budget constraints are not the main bottleneck. When the budget increased by 20%, the coverage rate rose from 16.49% to 23.58%, and the newly added locations were mainly concentrated in the subcentral areas.

Phase 2 demonstrates greater sensitivity to budget changes. A 20% increase in the budget raised the coverage rate from 44.73% to 52.88%, with an absolute increase of 8.15 percentage points. During this phase, the newly added locations are mainly distributed in the subcenters of cities. While location costs in these areas are relatively high, the demand density is also substantial. The expanded budget allows the model to prioritize these high-value locations.

The budget sensitivity in Phase 3 is most prominent. A 20% increase in the budget raised the coverage rate from 88.21% to 91.27%. Although the percentage change may seem insignificant, considering that the base coverage rate is already relatively high, the absolute increase in the actual covered population is very considerable. During this phase, the additional budget is primarily allocated to optimizing network coverage by selecting remaining high-cost sites that fill critical service gaps.

Notably, the impact of budget reduction on coverage shows nonlinear characteristics. In Phase 3, a 20% reduction in the budget decreases the coverage rate from 88.21% to 78.16% representing a substantial drop of 10.05 percentage points. This decline is significantly larger than the 3.06-percentage-point gain achieved by an equivalent budget increase, indicating the existence of a critical budget threshold for UAM network deployment. Below this threshold, a large number of high-value locations will not be selected, significantly reducing network efficiency.

### 5.3.2 Labor cost budgeting

The data in Table 7 show that the impact of the labor cost budget on demand coverage exhibits complex nonlinear characteristics and phased differences. In Phase 1, an increase of 10% in the labor cost budget raised the coverage rate from 16.49% to 20.46%. However, when the budget continued to increase to 20%, the coverage rate slightly dropped to 17.99%, presenting an inverted U-shaped rela-

tionship.

Under these constraints, a 20% increase in the labor cost budget surprisingly results in lower Phase 1 demand coverage compared to a 10% budget increase. This abnormal phenomenon occurs because, with a 10% budget increase, the algorithm achieves higher labor cost utilization (83.13%) by prioritizing locations with optimal demand-to-salary ratios, significantly boosting initial coverage. In contrast, the 20% budget increase leads to suboptimal location selection (71.68% utilization), excluding some ultra-high-demand locations that must then be compensated for in later phases - ultimately yielding similar global coverage despite the higher initial investment.

Phase 3 demonstrates the lowest sensitivity to labor cost budget adjustments. A 20% increase in the budget only slightly raised the coverage rate from 88.21% to 88.24%, with a very weak improvement effect. This is because the operational efficiency in the mature phase has reached a relatively high level, and network effects have reduced the impact of individual verti-port performance on overall system quality. This discovery holds significant implications for practical planning: in the later phase of UAM network construction, more resources can be allocated to land costs rather than labor costs.

### 5.3.3 Transportation cost budgeting

As shown in Table 8, the impact of changes in transportation accessibility indicators on demand coverage shows unique spatial distribution characteristics and temporal dynamics. In Phase 1, a 20% increase in the indicator raised the coverage rate from 16.49% to 20.99%, representing an increase of 4.5 percentage points. Analysis of the location selection results reveals that the lower demand coverage rate in Phase 1 is due to the preference for building more vertiports in central areas, while achieving higher demand coverage requires prioritizing vertiports in peripheral areas. However, the unmet demands will be addressed in subsequent phases. Therefore, overall, easing the constraints on transportation accessibility results in a monotonic increase in the demand coverage rate, though with some fluctuations in the early phases.

The Phase 3 results reveal the interaction between transportation accessibility and network density. When network coverage reaches a relatively high level, improvements in transportation conditions have a limited

**Table 7** Sensitivity analysis of labor cost budget

Phase	S1 (-20%)	S2 (-10%)	S3 (Base case)	S4 (+10%)	S5 (+20%)
Phase 1	19.64%	20.45%	16.49%	20.46%	17.99%
Phase 2	47.71%	52.06%	44.73%	50.12%	50.00%
Phase 3	82.99%	87.62%	88.21%	88.21%	88.24%

**Table 8** Sensitivity analysis of transportation accessibility

Phase	F1 (-20%)	F2 (-10%)	F3 (Base case)	F4 (+10%)	F5 (+20%)
Phase 1	15.14%	20.06%	16.49%	20.57%	20.99%
Phase 2	44.61%	48.28%	44.73%	49.42%	50.83%
Phase 3	85.69%	87.32%	88.21%	88.76%	88.89%

impact on the overall system. A 20% increase in the indicator only increased the coverage rate from 88.21% to 88.89%, representing an increase of less than 1 percentage point. This is because the dense network layout already provides good accessibility, further marginal improvements contribute minimally.

### 5.3.4 Regional sensitivity analysis

Based on the multi-phase construction data of vertiports in Shenzhen, this study systematically investigates the dynamic impacts of three key factors—namely, land cost, labor cost, and transportation accessibility — on the construction scale and temporal distribution of vertiports across administrative districts under varying budget constraints. By developing five sensitivity scenarios (including a 20% increase or decrease, a 10% increase or decrease, and a baseline level), this study reveals the region-specific response mechanisms under resource constraints.

Table 9 presents the dynamic responses of location construction across various districts to land cost variations of  $\pm 10\%$  and  $\pm 20\%$ . Overall, land cost fluctuations have a limited impact on the total construction volume in each district, but significant variations exist in their internal phase allocation.

In Futian District, when land costs increase, the number of Phase 3 locations rises from 7 to 10, indicating a shift of construction focus toward later phases under higher land costs. Nanshan District exhibits a similar trend: while the total locations in R3-R5 remain stable at 22-26, Phase 1 locations increase from 8 to 12, indicating prioritized early-phase construction.

In Guangming District, the total locations grow stepwise with land cost increases, rising from 5 in R1 to 11 in R5 (a 120% increase). Early-phase construction received lower priority, but with budget rises, later-phase locations increase significantly. As the district with the largest construction scale, Bao'an District displays high sensitivity to land cost constraints, with the total number of vertiport locations growing from 31 in R1 to 40 in R5. Conversely,

Longgang District's total locations drop from 24 to 18 when land costs rise, with Phase 3 locations decreasing from 13 to 9, reflecting stringent land budget constraints.

Peripheral areas such as Yantian, Pingshan, Dapeng New District maintain totals below 10 locations. However, when the budget increases, Yantian and Pingshan each gain one additional location, indicating their slight sensitivity to land costs. Analysis of vertiport locations indicates that clustering centers in Yantian are few and concentrated in tourist areas like Dameisha and Rose Coast, where land prices are relatively high. Notably, Luohu District's total remains stable (9-10 locations) despite land cost fluctuations. Yet, with budget increases, Phase 1 locations drop from 5 to 0, while Phase 2 rises from 1 to 6, indicating optimized land resource allocation via construction sequencing. Longhua District exhibits high adaptability, with totals stable at 19-21 and fewer than 3 fluctuations in location numbers across phases.

Table 10 shows that the impact of changes in labor costs on location construction presents regional heterogeneity.

The total number of locations in Futian District and Nanshan District remained stable at 19 and 22 respectively, but the internal phase adjustment was significant. In Nanshan District, the total number of locations only dropped to 19 when the labor cost decreased by 20%. Under standard conditions, the distribution of the number of locations built by phase in Futian District was relatively uneven. Only two locations were built in Phase 1. Increasing or decreasing the budget for labor costs can improve phase balance, but the total amount remains unchanged.

When a 20% reduction in the labor cost budget, Nanshan District only built two locations in Phase 1. By increasing the budget, the number of locations built in Phase 1 grew significantly to 6-9. The total volume in Bao'an District has remained stable at 35-37, and the proportion of Phase 3 has always exceeded 50%, reflecting its low sensitivity to changes in labor costs.

When the labor cost rose, the total amount in Longgang District and Longhua District increased from 18 to 21 and

**Table 9** District-wise vertiport construction under land cost variations

District	R1 (-20%)				R2 (-10%)				R3 (Base)				R4 (+10%)				R5 (+20%)			
	P1	P2	P3	A	P1	P2	P3	A	P1	P2	P3	A	P1	P2	P3	A	P1	P2	P3	A
Futian	5	6	5	16	7	4	7	18	2	8	9	19	6	6	7	19	5	4	10	19
Luohu	5	1	3	9	1	6	2	9	1	2	6	9	-	5	4	9	-	6	4	10
Yantian	-	-	-	-	-	1	-	1	-	-	1	1	-	-	2	2	-	1	1	2
Nanshan	4	4	6	14	3	5	9	17	8	8	6	22	11	7	8	26	12	6	8	26
Bao'an	4	11	16	31	4	12	17	33	7	11	19	37	3	12	25	40	6	18	16	40
Longgang	5	6	13	24	5	5	14	24	3	4	13	20	4	5	9	20	4	5	9	18
Longhua	5	6	8	19	5	5	10	20	7	4	9	20	3	9	8	20	3	6	11	20
Pingshan	1	2	1	4	2	2	2	6	1	2	3	6	-	3	4	7	-	4	3	7
Guangming 1		2	2	5	-	4	2	6	1	3	4	8	3	5	3	11	-	4	7	11
Dapeng	-	1	1	2	-	-	2	2	-	-	2	2	-	1	1	2	-	-	2	2

**Table 10** District-wise vertiport construction under labor cost variations

District	S1 (-20%)				S2 (-10%)				S3 (Base)				S4 (+10%)				S5 (+20%)			
	P1	P2	P3	A	P1	P2	P3	A	P1	P2	P3	A	P1	P2	P3	A	P1	P2	P3	A
Futian	5	7	7	19	4	8	7	19	2	8	9	19	5	8	6	19	5	5	9	19
Luohu	3	4	2	9	1	1	7	9	1	2	6	9	2	-	6	8	-	1	8	9
Yantian	-	-	-	-	-	-	-	-	-	-	1	1	-	-	1	1	-	-	1	1
Nanshan	2	9	8	19	9	7	6	22	8	8	6	22	6	8	8	22	6	10	6	22
Bao'an	8	6	19	35	7	12	18	37	7	11	19	37	6	11	20	37	8	13	15	36
Longgang	3	6	9	18	4	6	10	20	3	4	13	20	4	6	10	20	5	6	10	21
Longhua	8	6	5	19	2	7	11	20	7	4	9	20	5	6	10	21	3	6	12	21
Pingshan	-	1	2	3	1	4	1	6	1	2	3	6	-	4	2	6	1	2	4	7
Guangming	-	1	3	4	-	2	4	6	1	3	4	8	1	1	6	8	2	3	4	9
Dapeng	-	-	1	1	1	-	1	2	-	-	2	2	-	2	-	2	-	1	1	2

from 19 to 21 respectively, and the number in Phase 3 in Longhua District increased from 5 to 12. This indicates that the two districts have controlled the consumption of labor costs by delaying the construction period.

Guangming District has shown a prominent response to changes in labor costs, with the total amount increasing from 4 in S1 to 9 in S9, highlighting its high sensitivity to labor costs. Yantian District only deploys 1 vertiport under sufficient budgets, suggesting expansion potential. Despite increasing the budget for labor costs, Luohu District witnessed a decline in the total location amount. Although the total amount showed low sensitivity, there was a significant change within the period.

The total number of locations in Pingshan District and Dapeng New District has always been relatively low. In Pingshan District, the total number of locations only dropped from 6 to 3 when the budget was reduced by 20%, and remained basically stable at 6 in other circumstances.

Table 11 shows the impact of the adjustment of the transportation accessibility coefficient on the layout of vertiport locations.

The total volume in Futian District and Luohu District remains basically stable, and the changes in accessibility constraints are adapted to by optimizing the proportion of phases. When accessibility was relaxed in Nanshan District, the total number of vertiports dropped from 24 to 22. This reflects that under the condition of relaxed transportation accessibility constraints, the central area with better transportation conditions may sacrifice the construction of some vertiports. Bao'an District displays similar characteristics to Nanshan under these conditions.

Longgang District emerges as the most accessibility-sensitive region. Under the condition that the constraints on transportation accessibility are gradually relaxed, the total amount has increased from 15 in F1 to 29 in F5, from 8 to 14 in Phase 3, and from 5 to 11 in Phase 2, indicating that the improvement in accessibility has significantly released its construction potential.

The total volume fluctuation in Longhua District is relatively weak. Under the F1 condition, the proportion of vertiports built in Phase 3 in Guang-ming District is as high as 100%. Relaxing the transportation accessibility constraints can balance the number of locations built in

**Table 11** District-wise vertiport construction under transportation accessibility variations

District	F1 (-20%)				F2 (-10%)				F3 (Base)				F4 (+10%)				F5 (+20%)			
	P1	P2	P3	A	P1	P2	P3	A	P1	P2	P3	A	P1	P2	P3	A	P1	P2	P3	A
Futian	3	9	7	19	2	8	9	19	2	8	9	19	4	5	9	18	3	9	6	18
Luohu	3	1	5	9	1	2	6	9	1	2	6	9	2	1	6	9	3	2	4	9
Yantian	-	-	-	-	-	1	1	2	-	1	1	2	1	-	1	2	1	-	1	2
Nanshan	7	8	9	24	8	8	6	22	8	8	6	22	8	7	6	21	7	6	8	21
Bao'an	9	11	18	38	7	11	19	37	7	11	19	37	6	9	22	37	5	11	20	36
Longgang	2	5	8	15	3	4	13	20	3	4	13	20	5	9	12	26	4	11	14	29
Longhua	4	7	10	21	7	4	9	20	7	4	9	20	3	10	8	21	5	7	9	21
Pingshan	1	3	3	7	1	2	3	6	1	2	3	6	1	1	5	7	-	1	5	6
Guangming	-	-	8	8	1	3	4	8	1	3	4	8	-	3	4	7	1	1	5	7
Dapeng	1	-	1	2	-	-	2	2	-	-	2	2	1	1	-	2	2	-	-	2

different phases in Guangming District.

The total volume in Pingshan District, Dapeng New District and Yantian District has remained stable at a relatively low level, and there have been significant phase vacancies in Yantian District and Dapeng New District.

Based on the above analysis, it can be seen that the construction of vertiports in Shenzhen shows a distinct “core-edge” gradient response feature. Futian District and Nanshan District exhibit significant characteristics of “total rigidity - structural flexibility,” that is, they maintain the stability of the overall scale by optimizing the allocation of construction phases. Bao'an District and Longgang District, on the other hand, show a “scale adaptation type” response, with their total construction volume fluctuating significantly with changes in constraint conditions. In contrast, Yantian District and Dapeng New District are subject to hard constraints, resulting in a relatively small number of constructed vertiports. The proportion of “low demand - high cost” sites is relatively high. It is particularly worth noting that the impact of different cost factors on the construction sequence shows significant heterogeneity - the increase in land costs generally leads to a shift in the construction focus to later phases, the rise in labor costs makes it easier to compress the construction scale in the early phase, while the improvement in transportation accessibility can effectively activate the long-term development potential of the sub-central area.

### 5.3.5 Practical decision-making implications

Building upon the sensitivity analysis results, this study provides concrete decision-support recommendations for urban planners and UAM operators in real-world application scenarios.

#### (1) Land acquisition

The sensitivity analysis identifies land cost budget as the most critical factor influencing demand coverage. Accordingly, differentiated land acquisition strategies are recommended:

1) Core areas (e.g., Futian, Nanshan): Implement advance land banking strategies through long-term leasing or collaborative development models to control costs.

2) Sub-center areas (e.g., Bao'an, Longgang): Adopt flexible pricing mechanisms combining benchmark land prices with floating compensation schemes.

3) Peripheral areas (e.g., Dapeng, Yantian): Consider bundled development with tourism projects or emergency facilities to share costs and enhance viability.

#### (2) Phased deployment strategies

The analysis reveals phased and regionally heterogeneous sensitivities to different cost factors, suggesting the following deployment strategy:

1) Initial phase: Prioritize demonstration vertiports in core areas to achieve rapid return on investment through high demand density while collecting operational data.

2) Mid-term phase: Expand to sub-center areas, focusing on land cost control through modular and standardized construction approaches.

3) Mature phase: Complete network coverage in peripheral areas, emphasizing transportation accessibility improvements through coordination with local transportation renovation projects.

#### (3) UAM subsidy considerations

Given the nonlinear characteristics of cost sensitivities, a tiered subsidy policy is proposed:

1) Launch-phase subsidies: For high-demand but cost-sensitive core area vertiports, implement combined “construction subsidy and operational subsidy” packages to ensure project viability and encourage private investment.

2) Growth-phase incentives: For sub-center areas, introduce performance-based subsidies linked to passenger growth rates and service satisfaction metrics.

3) Maturation-phase transition: Gradually phase out direct subsidies, transitioning to indirect support mechanisms such as tax incentives or franchise arrangements.

## 6 Conclusions

This study develops a decision-support framework to optimize vertiport placement, thereby fostering the sustainable growth of the UAM. To achieve this, we first analyzed residents' travel mode choices using a multinomial logit model based on combined RP and SP survey data. The model estimates individual probabilities of choosing UAM services and identifies potential user groups through time value coefficients. We then employed the K-means algorithm to cluster OD points and developed a three-phase multi-objective integer programming model for vertiport location optimization, with the dual objectives of maximizing demand coverage and minimizing costs. A case study was conducted in Shenzhen to validate the feasibility of the proposed approach. Furthermore, a sensitivity analysis was performed to evaluate the impacts of land cost, labor cost, and transportation accessibility on the demand coverage rate.

The findings offer several managerial implications. First, UAM operators can leverage time value coefficients to precisely identify time-sensitive user groups, thereby optimizing service pricing and marketing strategies. Second, the proposed phased construction model provides an operational implementation plan for the gradual development of urban UAM infrastructure and offers urban managers a scientific method for UAM location selection. Finally, the sensitivity analysis results can guide urban managers in reasonably controlling key cost elements such as land cost, labor cost, and transportation accessibility. Particularly, the land cost budget was identified as the most influential factor affecting demand coverage rates.

This research has certain limitations. The valid samples obtained in this survey have certain limitations in demographic characteristics, and the sample representativeness and coverage require improvement. In addition, vertiport capacity constraints were not fully considered, and coordination with existing road networks was insufficiently analyzed. Notably, airspace safety constraints and flight corridor planning, which are critical for practical implementation, were not incorporated into the vertiport layout optimization. These limitations indicate the need for deeper research on vertiport layout optimization.

Future research on UAM system planning could explore the following key directions in depth. First, it is necessary to overcome the limitations of single data sources by building a multi-source data fusion framework that integrates mobile phone signaling data, social media geotags, and other data sets. Furthermore, using data assimilation technology to establish a comprehensive demand perception system, coupled with adopting multi-period dynamic planning combined with demand forecasting and technology evolution analysis, will enhance

the long-term adaptability of planning. Second, the geographical environment around potential vertiports should be evaluated using geographic information systems integrated with urban morphological parameters to accurately identify suitable areas for vertiport construction. Meanwhile, the connection efficiency between vertiports and the existing transportation network must be improved through a comprehensive assessment of the highway transportation network. This will not only optimize the feasibility of vertiport location selection but also achieve efficient coordination between UAM and ground transportation systems. Finally, based on UAM demand forecasts and vertiport placement solutions, research on airspace safety and flight corridor planning is urgently needed. Future studies should investigate: (1) multi-level dynamic airspace management models to design safe and efficient flight corridor networks; (2) risk assessment models along flight corridors, particularly for protecting densely populated areas and critical infrastructure; (3) integrated coordination mechanisms between airspace and ground transportation; (4) intelligent airspace management systems based on digital twin and artificial intelligence technologies; and (5) flight corridor design standards and policy frameworks adapted to urban environments. These investigations will provide essential technical support for the safe large-scale operation of UAM systems.

**Competing Interests** The authors declare that they have no competing interests.

**Open Access** This article is licensed under a Creative Commons Attribution 4.0 International License, which permits use, sharing, adaptation, distribution and reproduction in any medium or format, as long as you give appropriate credit to the original author(s) and the source, provide a link to the Creative Commons licence, and indicate if changes were made.

The images or other third party material in this article are included in the article's Creative Commons licence, unless indicated otherwise in a credit line to the material. If material is not included in the article's Creative Commons licence and your intended use is not permitted by statutory regulation or exceeds the permitted use, you will need to obtain permission directly from the copyright holder. To view a copy of this licence, visit <http://creativecommons.org/licenses/by/4.0/>.

## References

- Al Haddad C, Chaniotakis E, Straubinger A, et al (2020). Factors affecting the adoption and use of urban air mobility. *Transportation Research Part A, Policy and Practice*, 132: 696–712
- Ale-Ahmad H, Mahmassani H S (2021). Capacitated location-allocation-routing problem with time windows for on-demand urban air taxi operation. *Transportation Research Record: Journal of the Transportation Research Board*, 2675(10): 1092–1114
- Anania E C, Rice S, Walters N W, et al (2018). The effects of positive and negative information on consumers' willingness to ride in a driverless vehicle. *Transport Policy*, 72: 218–224

- Arthur D, Vassilvitskii S (2006). K-means++: The advantages of careful seeding. Stanford: Stanford University
- AutoNavi (2024). 2024 Q2 Traffic Analysis Report of Major Chinese Cities. Available at the website of AutoNavi official report center
- Bauranov A, Rakas J (2021). Designing airspace for urban air mobility: A review of concepts and approaches. *Progress in Aerospace Sciences*, 125: 100726
- Becker K, Terekhov I, Gollnick V (2018). A global gravity model for air passenger demand between city pairs and future interurban air mobility markets identification. In: 2018 Aviation Technology, Integration, and Operations Conference, 2885
- Boddupalli S S (2019). Estimating demand for an electric vertical landing and takeoff (eVTOL) air taxi service using discrete choice modeling. Dissertation for the Doctoral Degree. Atlanta: Georgia Institute of Technology
- Brunelli M, Ditta C C, Postorino M N (2023). SP surveys to estimate airport shuttle demand in an urban air mobility context. *Transport Policy*, 141: 129–139
- Chen L, Wandelt S, Dai W, Sun X (2022). Scalable vertiport hub location selection for air taxi operations in a metropolitan region. *INFORMS Journal on Computing*, 34(2): 834–856
- Cho S H, Kim M (2022). Assessment of the environmental impact and policy responses for urban air mobility: A case study of Seoul metropolitan area. *Journal of Cleaner Production*, 360: 132139
- Cohen A P, Shaheen S A, Farrar E M (2021). Urban air mobility: History, ecosystem, market potential, and challenges. *IEEE Transactions on Intelligent Transportation Systems*, 22(9): 6074–6087
- Coykendall J, Metcalfe M, Hussain A et al (2022). Advanced air mobility: Disrupting the future of mobility. Deloitte. Available at the website of Deloitte Insights
- Davis F D, Bagozzi R P, Warshaw P R (1989). User acceptance of computer technology: A comparison of two theoretical models. *Management Science*, 35(8): 982–1003
- Development and Reform Commission of Shenzhen Municipality (2024). Shenzhen High-Quality Construction Plan for Low-Altitude Infrastructure (2024–2026). Retrieved from the website of sz.gov.cn
- Du S, Zhong G, Wang F, et al (2025). A framework for collaborative UAM traffic flow optimization with mission preferences: Incorporating customized strategy synergy into strategic conflict management. *Transportation Research Part E, Logistics and Transportation Review*, 202: 104326
- Eker U, Fountas G, Anastasopoulos P Ch, et al (2020). An exploratory investigation of public perceptions towards key benefits and concerns from the future use of flying cars. *Travel Behaviour & Society*, 19: 54–66
- European Union Aviation Safety Agency (2022). Urban Air Mobility (UAM) operational rules proposal for air taxis. Available at the website of EASA official documents
- Falocchio J C, Levinson H S (2015). The costs and other consequences of traffic congestion. In: *Road Traffic Congestion: A Concise Guide*. New York: Springer, 159–182
- Goyal R, Reiche C, Fernando C, et al (2018). Urban Air Mobility (UAM) Market Study. NASA Report. Available at the website of NASA
- Hae Choi J, Park Y (2022). Exploring economic feasibility for airport shuttle service of urban air mobility (UAM). *Transportation Research Part A, Policy and Practice*, 162: 267–281
- Ilahi A, Belgiawan P F, Balac M, et al (2021). Understanding travel and mode choice with emerging modes; a pooled SP and RP model in Greater Jakarta, Indonesia. *Transportation Research Part A, Policy and Practice*, 150: 398–422
- Jiang G, Fan Q, Zhang Y, et al (2025). A tradable carbon credit incentive scheme based on the public-private partnership. *Transportation Research Part E, Logistics and Transportation Review*, 197: 104039
- Joby Aviation (2024). Joby completes first FAA testing on major aircraft aerostructure. Retrieved from the website of jobyaviation.com/news
- Lim E, Hwang H (2019). The selection of vertiport location for on-demand mobility and its application to Seoul metro area. *International Journal of Aeronautical and Space Sciences*, 20(1): 260–272
- Long Q, Ma J, Jiang F, et al (2023). Demand analysis in urban air mobility: A literature review. *Journal of Air Transport Management*, 112: 102436
- Merat N, Madigan R, Nordhoff S (2017). Human factors, user requirements, and user acceptance of ride-sharing in automated vehicles. *International Transport Forum Discussion Paper*. Paris: OECD Publishing
- Nadrian H, Taghdisi M H, Pouyesh K, et al (2019). “I am sick and tired of this congestion”: Perceptions of Sanandaj inhabitants on the family mental health impacts of urban traffic jam. *Journal of Transport & Health*, 14: 100587
- Rajendran S, Srinivas S (2020). Air taxi service for urban mobility: A critical review of recent developments, future challenges, and opportunities. *Transportation Research Part E, Logistics and Transportation Review*, 143: 102090
- Rajendran S, Zack J (2019). Insights on strategic air taxi network infrastructure locations using an iterative constrained clustering approach. *Transportation Research Part E, Logistics and Transportation Review*, 128: 470–505
- Rath S, Chow J Y J (2022). Air taxi skyport location problem with single-allocation choice-constrained elastic demand for airport access. *Journal of Air Transport Management*, 105: 102294
- Rimjha M, Hotle S, Trani A, Hinze N (2021). Commuter demand estimation and feasibility assessment for Urban Air Mobility in Northern California. *Transportation Research Part A, Policy and Practice*, 148: 506–524
- Rousseeuw P J (1987). Silhouettes: A graphical aid to the interpretation and validation of cluster analysis. *Journal of Computational and Applied Mathematics*, 20: 53–65
- Roy S, Kotwicz Herniczek M T, German B J, et al (2021). User base estimation methodology for a business airport shuttle air taxi service. *Journal of Air Transportation*, 29(2): 69–79
- Salama M, Srinivas S (2020). Joint optimization of customer location clustering and drone-based routing for last-mile deliveries. *Transportation Research Part C, Emerging Technologies*, 114: 620–642
- Thomas K, Granberg T A (2023). Quantifying visual pollution from urban air mobility. *Drones*, 7(6): 396

- Vascik P D (2017). Systems-level analysis of on demand mobility for aviation. Dissertation for the Doctoral Degree. Cambridge: Massachusetts Institute of Technology
- Wei L, Justin C Y, Mavris D N (2020). Optimal placement of airparks for STOL urban and suburban air mobility. AIAA Scitech 2020 Forum, 0976
- Wu Z, Zhang Y (2021). Integrated network design and demand forecast for on-demand urban air mobility. *Engineering*, 7(4): 473–487
- Yan Y, Wang K, Qu X (2024). Urban air mobility (UAM) and ground transportation integration: A survey. *Frontiers of Engineering Management*, 11(4): 734–758
- Zhou S, Guo Z, Chen J, et al (2025a). Large containership stowage planning for maritime logistics: a novel meta-heuristic algorithm to reduce the number of shifts. *Advanced Engineering Informatics*, 64: 102962
- Zhou S, Liu X, Chen J, et al (2025b). Joint optimization of slot and empty container co-allocation for liner alliances with uncertain demand in maritime logistics industry. *Transportation Research Part E, Logistics and Transportation Review*, 204: 104437
- Zhuo X, Sun Y, Zhou S (2025). Impact of consumers traceability awareness on blockchain adoption in supply chains. *IEEE Transactions on Engineering Management*, 72: 1140–1153